Atmospheric and
Environmental Research, Inc.

Algorithm Theoretical Basis Document (ATBD)
for the
Conical-Scanning Microwave Imager/Sounder (CMIS)
Environmental Data Records (EDRs)

Volume 13: Surface Temperature EDRs

Covering: Land Surface Temperature EDR
Ice Surface Temperature EDR

Version 1.0 – 15 March 2001

Solicitation No. F04701-01-R-0500

Submitted by:
Atmospheric and Environmental Research, Inc.
131 Hartwell Avenue
Lexington, MA 02421-3126

With contributions by:
John Galantowicz, Jennifer Hegarty, Sid Boukabara, Richard Lynch, Alan Lipton, Jean-Luc Moncet, Helene Rieu-Isaacs, Xu Liu, Ned Snell

Prepared for:
Boeing Satellite Systems
919 Imperial Highway
El Segundo, CA 90245

This page intentionally left blank.

REVISION HISTORY

Version	Release Date	POC	Comments
1.0	6 Feb., 2001 (PDR)	Galantowicz	Initial partial draft release.

RELATED CMIS DOCUMENTATION

Government Documents

Title	Version	Authorship	Date
CMIS SRD for NPOESS Spacecraft and Sensors	3.0	Associate Directorate for Acquisition NPOESS IPO	2 March 2001

Boeing Satellite Systems Documents

Title		Covering
ATBD for the CMIS TDR/SDR Algorithms		
ATBD for the CMIS EDRs	Volume 1: Overview	Part 1: Integration
		Part 2: Spatial Data Processing • Footprint Matching and Interpolation • Gridding • Imagery EDR
	Volume 2: Core Physical Inversion Module	
	Volume 3: Water Vapor EDRs	Atmospheric Vertical Moisture Profile EDR Precipitable Water EDR
	Volume 4: Atmospheric Vertical Temperature Profile EDR	
	Volume 5: Precipitation Type and Rate EDR	
	Volume 6: Pressure Profile EDR	
	Volume 7: Cloud EDRs	Part 1: Cloud Ice Water Path EDR
		Part 2: Cloud Liquid Water EDR
		Part 3: Cloud Base Height EDR
	Volume 8: Total Water Content EDR	
	Volume 9: Soil Moisture EDR	
	Volume 10: Snow Cover/Depth EDR	
	Volume 11: Vegetation/Surface Type EDR	
	Volume 12: Ice EDRs	Sea Ice Age and Sea Ice Edge Motion EDR Fresh Water Ice EDR
	Volume 13: Surface Temperature EDRs	Land Surface Temperature EDR Ice Surface Temperature EDR
	Volume 14: Ocean EDR Algorithm Suite	Sea Surface Temperature EDR Sea Surface Wind Speed/Direction EDR Surface Wind Stress EDR

Title		Covering
	Volume 15: Test and Validation	All EDRs

Bold = this document

TABLE OF CONTENTS FOR VOLUME 13

LIST OF TABLES

LIST OF FIGURES

1. Abstract

The CMIS Land Surface Temperature (LST) and Ice Surface Temperature (IST) EDRs will be retrieved by a globally consistent algorithm built primarily on the atmospheric Core Module's surface temperature (or skin temperature) retrieval product. The Core Module retrieves surface temperature as a part of the solution state for an surface-atmosphere radiative transfer model. The Core Module reports surface temperature at both the 50 and 25 km HCS of the LST and IST EDRs, respectively, using brightness temperatures inputs at the corresponding spatial resolutions. The LST EDR is equivalent to the Core Module's surface temperature product; it will be reported over global land cells as well as sea ice-covered ocean cells such that the LST and SST products may together provide a seamless, global surface temperature product with 50 km nominal HCS. The IST EDR is equivalent to the Core Module's surface temperature product over land ice; over sea ice, the surface temperature algorithm derives ice concentration estimates from Core Module-derived surface emissivities and uses them to derive ice temperature from the mean-cell surface temperatures provided by the Core Module. Global LST EDR measurement precision (standard error) and accuracy (mean bias) are expected to be better than 2.5 K and 0.5 K, respectively. IST EDR measurement uncertainty (mean squared error) is expected to be better than 3 K.

2. Introduction

2.1. Purpose

The purpose of this document is to provided all the information necessary to understand, operate, further develop, and use the products from the CMIS surface temperature (ST) retrieval algorithm. The CMIS SRD (NPOESS IPO, 2000) specifies the EDRs' required (threshold level) operational and performance characteristics including definitions, spatial resolution, and measurement range and uncertainty. The integrated ST algorithm (Core Module plus mixed cell corrections for IST based on fresh water ice and sea ice concentration inputs) meets its nominal performance specifications by deriving all of its products from CMIS brightness temperature observations. Furthermore, the algorithm reports additional products that extend the retrieval capabilities and aid quality control.

Section 3 summarizes the EDR requirements either specified in the SRD or derived from it. It contains a historical background and physical basis for the proposed algorithm, and it describes the instrument characteristics and data from all sources necessary to meet NPOESS requirements.

Section 4 describes the physical parameterizations relevant to the surface typing algorithm. We also provide algorithm processing flow diagrams including dependencies within the overall processing flow and list input and output fields and ancillary databases.

Section 5 real-data test results and provides measurement uncertainty and other performance estimates based on the tests. These tests are used to demonstrate that the algorithm products will meet its nominal predicted performance specifications. We describe the environmental conditions under which we expect the retrievals to meet requirements, not to meet requirements, or to degrade substantially. We also summarize special constraints, limitations, or assumptions made in algorithm parameterization or testing that may limit the algorithm's applicable domain or necessitate post-launch adjustments based on specific systematic contributions in order to meet performance estimates.

Section 6 discusses algorithm calibration points and outlines the steps necessary to transition algorithm operation from heritage-data to CMIS-data inputs. We outline considerations for pre-

and post-launch calibration and validation efforts, including needed measurement capabilities and hardware, field measurements, and existing sources of truth data.

Section 7 describes practical considerations including numerical computation considerations, algorithm quality control and diagnostics, exception and error handling, and archival requirements.

2.2. Document Scope

The *ATBD for the CMIS Vegetation/Surface Type EDR* covers algorithm operations beginning with the ingestion of earth-gridded Core Module products (surface effective broad-band atmospheric window-channel emissivities) and the earth-gridded snow and ice detection flag, and concluding with reporting of the retrieved type and other related algorithm products on the same earth-grid. Preceding sensor data processing steps are covered in the *ATBD for SDR Processing*, *ATBD for the Core Physical Inversion Module,* and *ATBD for the Snow Cover/Depth EDR* (AER, 2000). This ATBD provides outlines for continued algorithm development and advancement and for pre- and post-launch calibration/validation efforts. These outlines are intended to be reviewed and revised prior to launch as new data sources and research become available.

3. Overview and Background Information

3.1. Objectives of the surface temperature retrievals

The LST and IST EDRs are specific measurements that CMIS must perform to complete the mission objectives stated in the SRD: "The mission of CMIS is to provide an enduring capability for providing measurements on a global basis of various atmospheric, land, and sea parameters of the Earth using microwave remote sensing techniques. The CMIS instrument will collect relevant information from a spaceborne platform, and utilize scientific algorithms to process that information on the ground into designated [EDRs]." (SRD, section 3.1.7)

3.2. Objectives of the Land Surface Temperature EDR retrieval

The SRD requires that CMIS retrieve land surface temperature at 50 km HCS over all land (non-ocean) areas of the globe. Additionally, the CMIS ST algorithm will provide 50 km surface temperature for areas of ocean covered with sea ice such that LST and SST will together comprise a 50 km HCS seamless global surface temperature product. The CMIS atmospheric Core Module does the bulk of the ST algorithm LST retrieval work when it derives surface temperature (also referred to as skin temperature T_{skin} or effective emitting temperature T_{eff}) along with the other components of its earth-atmosphere radiative transfer model. The Core Module retrieves T_{eff} from 50 km HSR composite CMIS brightness temperatures. A gridding module then maps surface temperature to an earth-grid. The ST algorithm module packages gridded surface temperatures as the LST EDR and applies quality control checks. Because the Core Module's T_{eff} is the aggregate temperature over the retrieval cell, LST aims to represent the cell-average temperature in cells having a mixture of surfaces—dry, flooded, barren, vegetated, water bodies, snow, or ice.

The CMIS LST product will be useful as a key measure of long-term climatological and real-time meteorological state. With CMIS data available from two or more sun-synchronous platforms, temporal sampling of LST may be more than 4 times per day. The data may be used as inputs or validation for global climate models or regional hydrological or weather models. Note that the Core Module-retrieved T_{eff} is available at every CMIS HCS—50, 40, 25, 20, and 15 km—in both the sensor (scan-track) reference frame and earth-gridded. These could be useful

for higher-resolution applications and as complements to the EDR retrievals at the corresponding resolutions.

CMIS LST will complement near-simultaneous VIIRS LST EDR measurements. The VIIRS LST is required at 1-4 km HCS and will be available only for clear sky conditions. VIIRS temporal sampling may be more than 6 times per day due to VIIRS wider swath and its planned installation on three NPOESS platforms.

3.3. Objectives of the Ice Surface Temperature EDR retrieval

The SRD requires that CMIS retrieve ice surface temperature at 30 km HCS over ice-covered land and water areas of the globe. The CMIS ST algorithm will provide the IST product at 25 km HCS, which has the advantages of being half the LST HCS while eliminating 30 km HCS processing altogether. As with LST, the CMIS atmosphere Core Module derives cell-aggregate T_{eff} over ice along with the other radiative transfer model terms. (We will use the T_{eff} designation for ST retrievals because the term "skin temperature" is especially misleading for the ice emission problem in which microwave penetration depths are typically both large and frequency-dependent.) For IST over land ice, T_{eff} processing follows the same procedure as LST: A gridding module maps T_{eff} to an earth grid and the ST algorithm module packages the IST EDR and applies quality control. For IST over water, the ST algorithm makes sea ice and fresh water ice concentration estimates and uses them to adjust the earth-gridded surface temperature to more closely represent the temperature of ice in the cell.

IST will be valuable in monitoring dynamic processes in land and water ice. Frequent sampling at high latitudes may be used to reduce measurement random errors by calculating daily mean temperatures. The data may be used as inputs or validation for climate and ice extent forecast models. IST is complementary to LST: It is reported smaller cells (25 km vs. 50 km for LST) and represents just the temperature of the ice portion of cells with ice-water mixtures whereas LST represents the cell-average temperature.

CMIS IST will complement near-simultaneous VIIRS IST EDR measurements. VIIRS IST may be retrieved in cells as small as 1-4 km and will be available only for clear sky conditions. Because VIS-IR ice penetration depths are significantly smaller than many microwave depths, measurements from both instruments may be used in conjunction to provide additional information on ice temperature gradients and ice-atmosphere heat transfer.

3.4. Summary of EDR requirements

3.4.1. SRD Requirements

The text and tables below are the portions of CMIS SRD section 3.2.1.1.1.1 that apply directly to the ST algorithm. Shading indicates attributes not addressed at all in this document.

> **Land Surface Temperature** **TRD App D Section 40.6.1**
> Land surface temperature (LST) is defined as the aggregate temperature of all objects comprising the land surface.

Table 3-1: SRD Requirements for the Land Surface Temperature EDR

Para. No.		Thresholds	Objectives
C40.6.1-1	a. Horizontal Cell Size	50 km	1 km
C40.6.1-2	b. Horizontal Reporting Interval	50 km	1 km
C40.6.1-3	c. Horizontal Coverage	Land	Land
C40.6.1-4	d. Measurement Range	213 K - 343 K	213 K - 343 K
C40.6.1-5	e. Measurement Accuracy	2.5 K	1 K
C40.6.1-6	f. Measurement Precision	0.5 K	0.025 K
C40.6.1-7	g. Mapping Uncertainty	5 km	1 km
C40.6.1-8	h. Swath Width	1700 km	3000 km (TBR)

Ice Surface Temperature **TRD App D Section 40.7.3**

This EDR is required under clear and cloudy conditions. As a threshold, the temperature of the surface of ice over land or water is required. The objective is to measure the atmospheric temperature 2 m above the surface of the ice.

Table 3-2: SRD Requirements for the Ice Surface Temperature EDR

Para. No.		Thresholds	Objectives
C40.7.3-1	a. Horizontal Cell Size	30 km	10 km
C40.7.3-2	b. Horizontal Reporting Interval	30 km	10 km
C40.7.3-3	c. Horizontal Coverage	Ice-covered land/water	Ice-covered land/water
C40.7.3-4	d. Measurement Range	213-275 K (ice surface)	213-293 K (2m above ice)
C40.7.3-5	e. Measurement Uncertainty	1 K	(TBD)
C40.7.3-6	f. Mapping Uncertainty	3 km	1 km
C40.7.3-7	g. Swath Width	1700 km (TBR)	(TBD)

In addition to these requirements, the SRD specifies:

1. "Science algorithms shall process CMIS data, and other data as required, to provide the [EDRs] assigned to CMIS." (SRD, paragraph SRDC3.1.4.2-1)
2. "Specified EDR performance shall be obtained for any of the orbits described in paragraph 3.1.6.3 …" (SRDC3.1.6.3-2)
3. "As a minimum, the EDR requirements shall be satisfied at the threshold level." (SRDC3.2.1.1.1-3)
4. "… the contractor shall identify the requirements which are not fully satisfied, and specify the conditions when they will not be satisfied." (SRCD3.2.1.1.1-4)
5. "… CMIS shall satisfy the EDR Thresholds associated with cloudy conditions under all measurement conditions …" (SRD SRDC3.2.1.1.1.1-1)

Also note that the CMIS system consists "of all ground and spaceborne hardware and software necessary to perform calibrated, microwave radiometric measurements from space and the software and science algorithms necessary to process … these measurement into a format consistent with the requirements of the assigned [EDRs]." (SRD, section 3.1.1)

3.4.2. Requirements interpretations

We infer the following statements as either direct consequences or clarifications of the SRD requirements stated above and take them as requirements to be satisfied by the ST algorithm or to be addressed through algorithm performance evaluation:

1. LST is the cell-average (aggregate) temperature regardless of the mix of surface types in the cell (e.g., dry land, flooded land, water bodies, snow cover, ice).

2. IST is the temperature averaged over the ice surfaces in the cell. Specifically, where IST is retrieved over water and open water comprises a portion of the cell, then IST is intended to represent the temperature of only the ice portion of the cell.
3. As discussed in the *CMIS ATBD Overview*, we assume for LST EDR performance evaluation purposes that the Measurement Accuracy requirement (2.5 K threshold) applies to the measurement standard error (random noise) and that the Measurement Precision requirement (0.5 K) applies to the measurement mean error (bias). In this document, measurement accuracy is defined as the mean bias between measurements and truth and measurement precision is defined as the standard error (square-root of the mean squared error with mean bias removed). To keep these assumption clear and internally consistent, where we state estimates for measurement accuracy we also state that the requirement is <0.5 K; and where we state estimates for measurement precision we state that the requirement <2.5 K.

3.4.3. Derived requirements on the surface temperature algorithm

We do not directly derive any requirements on the surface temperature algorithm from the requirements of other EDR algorithms. In order to provide a seamless global temperature product at 50 km HCS, we require that LST horizontal coverage be complementary to SST coverage. That is, the ST algorithm will derive 50 km LST for solid land surfaces and inland water bodies as well as for *areas of the oceans with sea ice cover*. The SST algorithm will derive 50 km (nominal) SST for areas of the oceans without sea ice cover such that LST and SST will comprise a 50 km global ST product.

3.5. Historical and background perspective of proposed algorithm

Previous studies have shown that the accuracy surface temperature (ST) retrievals from microwave brightness temperature may be better in practice than predicted from physical theory owing to the fact that competing environmental signals—e.g., due to surface emissivity and atmospheric emission and attenuation—have significant correlations in microwave channels. Experience in the last decade with SSM/I has shown that linear and non-linear regression-type retrieval models applied to a limited range of surface types can produce LST with uncertainties in the 2-2.5 K range (McFarland et al., 1990; Njoku, 1995). (Microwave LST algorithms are typically calibrated and validated against 2 m local shelter height air temperature measurements. If spatially representative skin temperatures were used instead, better performance might be achieved.) Bassist et al. (1998) reported 2 K error for 1°-gridded monthly-mean maximum temperature in tests with an empirically tuned algorithm that adjusts its emissivity parameterization as a function of detected wetness, snow, vegetation, and quartz surface characteristics. (Emissivity is used here as a proportionality constant between brightness temperature and surface temperature such that it explicitly incorporates otherwise neglected atmospheric effects.) Williams et al. (2000) generalizes this emissivity parameterization such that it may be calibrated to any surface type classified from brightness temperature observations with arbitrary functional form. Using parameterizations derived from linear regression of SSM/I measurements against (primarily) Eastern United States shelter height temperature, they report training data residual standard deviations between 2.4 and 4.3 K.

Physical-model based retrieval methods have limited application with SSM/I data because only one channel set (19V and 22V) samples an atmospheric absorption feature. Weng and Grody (1998) report LST retrieval uncertainties ranging from 3.8 K (simulated measurements) to 4.4 K (SSM/I measurements) in tests with a physical retrieval model based on the differing atmospheric absorption characteristics at 19.35 and 22.235 GHz. They assume that 19V and

22V emissivities are identical. (Atmospheric absorption is about as strong at 85 GHz as 22 but 85 GHz emissivity is harder to constrain without a nearby channel with a clearer view of the surface.) Many of their observations are relevant to the CMIS physical retrieval approach:

- The radiative transfer model is solved by a Newtonian iterative process using $T_s = T_B(85V)/e(85V)$ as a first guess solution for LST, where $e(85V) = 0.955$. In SSM/I data tests over grasslands, the first guess is correlated to shelter height air temperatures with an RMS error of 6.22 K. First guess errors for scattering cases (snow cover or precipitation) are generally larger than other cases.
- Solution of the physical model improves upon the first guess in both the non-scattering cases and many of the scattering cases, suggesting that the physical model may accurately retrieve LST in many cases identified from brightness temperatures as scattering. Poor convergence of some scattering cases may be due to failure of the model to recover from large biases in the first guess or atmospheric moisture too low to satisfy physical model requirements.
- Larger measurement errors observed in practice may be due to surface-air temperature differences, lack of spatial representativeness of the shelter temperatures, and high sensitivity of the 19-22 model to SSM/I instrument calibration and data processing.

The key role that that 22V channel plays in SSM/I retrievals of LST is highlighted both by the Weng and Grody physical model and the regression model results: Both the McFarland et al. (1990) and Williams et al. (2000) regression models heavily weight 22V brightness temperatures. In fact, for the "vegetated dry land" class, the Williams model is based solely on 22V data ($T_s = T_B(22V)/e_0(22V)$ where $e_0(22V) = 0.939$). In these models, the correlation of atmospheric signals due to temperature and water vapor to LST must be high enough to justify dependence on a non-window SSM/I channel with lower direct sensitivity to surface temperature. As discussed below, CMIS includes channels with a wider range of surface and atmospheric sensitivities than SSM/I. The CMIS ST algorithm coordinates its LST solution with the retrieval of atmospheric parameters such that the radiative transfer model forward calculation of brightness temperatures converges on the measurements simultaneously in all channels. In other words, the method provides a framework that can tie together inter-channel correlated atmospheric and surface signals and thereby isolate the effects that LST and other modeled phenomenon have on measured brightness temperatures.

Experience from heritage algorithms suggests that ice surface temperature (IST) retrieval is particularly challenging, especially for sea ice. Analytical methods provide approximate uncertainty estimates for the 6.7 GHz NASA Team Algorithm (Gloersen et al., 1993; Steffen et al., 1992): At 100% ice concentration, 4% ice concentration measurement uncertainty, 0.96 ice emissivity, and 0.02 emissivity uncertainty, IST uncertainty is 7.3 K; if ice concentration measurement uncertainty is 0, IST uncertainty drops to 5.7 K. To reach 1 K IST error with this method requires 0.003 emissivity uncertainty. Real-data algorithm tests also provide benchmark performance estimates. Tests comparing retrievals from the SMMR NASA Team Algorithm to wintertime high-Arctic AOBP buoy interior temperature over an 8-year period yielded measurement uncertainties of 4.1 K, including linear bias correction applied to better fit retrievals to data (Gloersen et al., 1993). And tests comparing retrievals from the SSM/I St. Germain and Comiso (1997) algorithm to AVHRR-derived surface temperatures resulted in uncertainties ranging from 2.1-4.6 K for 3 clear-sky scenes localized to the Bering Strait. We conclude from these analytical and experimental results that heritage retrievals are good to about 4 K generally with better performance possible where algorithm calibration and local conditions

best correspond. The limiting factors appear to be ice concentration measurement uncertainty and natural variability in ice emissivity.

3.6. Physics of Problem

The *CMIS Core Module ATBD* fully describes the radiative transfer (forward) model used to predict CMIS measurements given specified values for the atmospheric and surface state variables—that is, atmospheric pressure, temperature, moisture, and cloud water profiles and surface temperature and spectral emissivity. This discussion will focus on the aspects of the model that are most important in LST retrieval. The model treats the atmosphere as a plane-parallel non-scattering medium. Under the Rayleigh-Jeans approximation, the model's radiative transfer equation for brightness temperature $T_{B\nu}$ at frequency ν is:

$$T_{B\nu} \cong e_\nu T_{eff} \mathrm{T}_{s,\nu} + \int_{p_s}^{0} \Theta(p) \frac{\partial \mathrm{T}_\nu(p,\theta_u)}{\partial p} dp + (1-e_\nu)\mathrm{T}_{s,\nu}\left[\int_{0}^{p_s} \Theta(p) \frac{\partial \mathrm{T}^*_\nu(p,\theta_d)}{\partial p} dp + \mathrm{T}^*_\nu(0,\theta_d)\Theta_c\right] \quad (1)$$

where $\Theta(p)$ the atmospheric temperature at pressure-level p, $\mathrm{T}_\nu(p,\theta_u)$ (uppercase τ) is the total transmittance due to molecular species and cloud liquid water from pressure-level p to the top of the atmosphere ($p = 0$), θ_u is the viewing angle at which up-welling radiation is sensed, $\mathrm{T}^*_\nu(p,\theta_d)$ is the transmittance from pressure-level p to the surface at down-welling angle θ_d, e_ν is the surface emissivity, and Θ_c is the cosmic radiation term (2.73 K). The surface is treated as specularly reflective such that $\theta_u = \theta_d$ and surface reflectivity $r_\nu = 1 - e_\nu$.

In simple terms, the iterative solution to (1) converges when the brightness temperatures modeled with the current iteration's state estimate match the measurements at all the CMIS channels. (See the *CMIS Core Module ATBD* for more details on the solution method and convergence criteria.) For T_{eff} to be accurately retrieved with this formulation, both e_ν and $\mathrm{T}_{s,\nu}$ must also be well-resolved, on average, across all the channels. The second and third terms of (1)—representing upwelling and reflected/transmitted downwelling radiation—provide e_ν and T_ν sensitivity independent of T_{eff}, making it possible to resolve each of these variables under the right conditions. The remainder of this section focuses on what conditions are necessary and optimum for accurate T_{eff} measurement from multi-channel observations.

As discussed above, the primary focus of previous studies of LST retrieval from microwave observations has been on emissivity constraint, which has been achieved either through empirical calibration or, in the case of a 19-22 GHz physical retrieval, model formulation. (We refer to a condition as a constraint here if it provides a way to minimize the error contribution of a parameter in the LST retrieval or the state solution overall. A means of either independently estimating a parameter in real time or assuming prior knowledge of the parameter to the LST retrieval are special cases where the constraint is particularly strong.) Consider the following simplifications of (1) where T_{Bs} is the surface-emitted brightness temperature and T_{UP} and T_{DN} are the up- and down-welling terms, respectively:

$$T_B = T_{Bs}\mathrm{T}_s + T_{UP} + rT_{DN}\mathrm{T}_s \quad (2)$$

$$T_B = T_{eff}\mathrm{T}_s + T_{UP} - r(T_{eff} - T_{DN})\mathrm{T}_s\,. \quad (3)$$

T_B sensitivity to surface reflectivity (and emissivity) anomalies is highest when $|T_{eff} - T_{DN}|$ and atmospheric transmittance T_s are large. However, T_{eff} and e would be least independent were these conditions to prevail in all channels—that is, T_{eff} and channel-correlated e anomalies would be indistinguishable. If the channel set has a range of surface sensitivities, then T_{eff} and e can be decoupled provided that the algorithm applies sufficient constraint *between* emissivities at the various channels. Again, the 19-22 physical retrieval is a special case where emissivity is constrained to be equal for a single window-sounding channel pair. In the Core Module's more general formulation, we can combine multiple window and sounding channels that span the full atmospheric transmittance range (~0-1) and use a looser statistical constraint on emissivity that penalizes inter-channel differences according to *a priori* covariance data. Then a *single* T_{eff} (and atmospheric profile) solution must satisfy the measurement-model convergence criteria at *all* channels, and each channel's emissivity must balance surface emission and T_{DN} reflection terms within the inter-channel covariance penalty constraint. Using this formulation for LST and IST requires that the CMIS channel set must cover the atmospheric transmittance range for cold, dry, thin atmospheres as well as for moist, thick atmospheres. In fact, the CMIS sounding channels at 22, 50-60, and 183 GHz fulfill that requirement (discussed in more detail in *ATBD for the Core Module*).

Ice-water mixed cells

In cells with a mixture of water and ice surface cover, the surface temperature algorithm is required to report the mean temperature across the cell for LST and, for IST, the mean temperature across only the ice-covered portion of the cell. Consider a cell with N surface cover components with effective emitting temperature T_i and emissivity e_i covering f_i fractions of the cell. In a typical ice-water scene where T_i are not equivalent, it is impossible to completely separate emitting temperature and emissivity terms. Expanding T_{Bs} in equation (2), we have

$$T_B = \left[\overline{T}e + \sum \Delta T_i f_i e_i \right] \mathrm{T}_s + T_{UP} + r T_{DN} \mathrm{T}_s \tag{4}$$

where

$$r = \sum_{i=1}^{N} f_i r_i \tag{5}$$

is the f-weighted average scene reflectivity, $e = 1 - r$, $\overline{T}$ is the f-weighted average scene temperature and ΔT_i is the deviation of component i around $\overline{T}$. For a particular channel, the Core Module physical model describes one emissivity ($e_m = 1 - r_m$) and one temperature T_m which nominally have the following relationship to the surface emission terms in (4):

$$T_m e_m = \overline{T}e + \sum \Delta T_i f_i e_i \ . \tag{6}$$

Assuming emissivity sensitivity is dominated by atmospheric reflection such that e_m is retrieved accurately as $1 - r$ (neglecting measurement noise), then the retrieved value for T_m will approximate $\overline{T}$ as:

$$T_m = \overline{T} + \frac{\sum \Delta T_i f_i e_i}{e} \ . \tag{7}$$

As noted in the *ATBD for Ice EDRs*, this is the desirable scenario for ice concentration retrieval because e is retrieved most accurately. However, (7) suggests a limit on the accuracy of the surface temperature retrieval depending on which channels have the highest weight in the surface temperature solution. For example, given a 50/50 split scene consisting of first-year ice (FY) and open water (OW) with T_{FY} = 263 K and T_{OW} = 273 K, the $\overline{T}$ error represented by (7) is roughly between -0.2 K (37V) and -2 K (19H). (See the *ATBD for Ice EDRs* for ice type emissivity assumptions). Conversely, if the surface were sensed through the emission term only—that is, with no atmosphere—and $T_m = \overline{T}$ by algorithm definition (achieved through tuning, for example), then e_m is related to the true f-weighted emissivity as:

$$e_m = e + \frac{\sum \Delta T_i f_i e_i}{\overline{T}}. \tag{8}$$

Given the same FY-OW scene, the e error in (10) is between -0.0006 (37V) and -0.004 (19H).

The ST algorithm will use the Core Module's solution for $\overline{T}$ and emissivity-based estimates of the f_i to estimate IST for mixed ice-water cells. Given *a priori* mean values for the emissivities of first year and multi-year (MY) ice and open water and an assumed or nearby retrieved value for open water temperature T_{w0}, then the algorithm estimates the mean ice temperature as:

$$T_{ice} = \frac{e_m T_m - f_w e_w T_{w0}}{f_{FY} e_{FY} + f_{MY} e_{MY}}. \tag{9}$$

Since the derivation of (9) assumes that T_m is an unbiased estimate of $\overline{T}$, T_{ice} will be biased if the T_m - $\overline{T}$ relationship is better approximated by (7) some or all the time. Consequently, it will be necessary to reexamine (9) or apply an empirical correction to it based on data obtained during calibration/validation operations. For example, depending on the degree of correlation between e_m and T_m measurement errors, T_{ice} errors may be lower if e_m is replaced by an approximation consistent with the mixing model formulation: $e = f_{FY}e_{FY} + f_{MY}e_{MY} + f_w e_w$.

Surface temperature gradients

A second source of IST retrieval uncertainty is the effect of unequal effective sensing depths at the various CMIS channels and the presence of vertical temperature gradients in the ice. Pure ice is a highly transparent medium at microwave frequencies due to it's low loss factor which increases with frequency. The effective emitting temperature of the ice is a weighted integral over the ice vertical temperature profile similar to atmospheric temperature weighting functions. Because ice and snow have low thermal conductivity, they can support large (up to ~10 K/m) temperature gradients even when heat transfer rates are low. Consequently, lower frequencies can have effective emitting temperatures that differ by several degrees from those at higher frequencies.

Some biases in IST due to surface temperature gradients may be removed using empirical corrections based on data from calibration/validation operations. Temperature gradients in sea ice are typically negative (decreasing temperature toward the surface) due to the relative warmth of the 273 K water below and the lack of a strong diurnal cycle to support transient gradients. Land ice gradients may be positive or negative depending on season. Temperature gradient errors may be reduced overall by retrieving T_{eff} using only the highest frequencies required, or, similarly, by using high and low frequencies while loosening the constraints on the low

frequencies such that they contribute little to T_{eff} retrieval. Since the combination of 36 and 89 GHz window channels and the 50-60 GHz sounding channel family is a key to accurate surface temperature retrieval (for example, see section 5.3) 36 GHz is a good candidate lower frequency limit for minimizing temperature gradient errors. Further channel trades in this area will be based on test retrievals with algorithm calibration data.

3.7. Instrument characteristics and derived requirements

CMIS is a conically-scanning microwave radiometer with window channels—frequencies chosen to avoid atmospheric absorption lines—around 6, 10, 19, 37, and 88 GHz and atmospheric sounding channel families around 23, 50-60, 60, 166, and 183 GHz. The instrument rotates continuously at 31.6 rpm on an axis perpendicular to the ground taking observations along nearly semi-circular arcs centered on the satellite ground track. Successive arcs scanned by a single sensor channel are separated by about 12.5 km along-track (depending on satellite altitude.) Calibration data is collected from a source (hot) and deep-space reflector (cold) viewed during the non-earth-viewing portion of the rotation cycle. Each observation (or sample) requires a finite sensor integration time which also transforms the sensor instantaneous field of view (IFOV)—the projection, or footprint, of the antenna gain pattern on the earth—into an observation effective field of view (EFOV). The start of each sample is separated by the sample time which is slightly longer than the integration time. The sample time is t_s = 1.2659 ms for all channels with the exception of 10 GHz (exactly $2t_s$) and 6.8 GHz ($4t_s$). All samples fall on one of three main-reflector scan-arcs or a single secondary-reflector scan arc (166 and 183 GHz channels only).

Sensor sample processing (described in the *ATBD for Common EDR Processing Task*, AER, 2000) creates composite measurements which are the spatial weighted superposition of a contiguous group of sensor samples. Although not exact, the process is designed to match observations from different channels to a single reference footprint: The composite fields-of-view (CFOVs) from different channels are more closely matched and collocated than the corresponding EFOVs. In addition, because sensor noise (as measured in NEDT) is both random and independent between samples, the effective NEDT of composite footprints may be reduced (amplified) if the square-root of the sum of squared sample weights is less than (greater than) one. The surface temperature algorithm uses data processed to match 50x50 km (for LST) and 25x25 km (for IST) reference footprints.

Table 3-3 lists specific characteristics relevant to the LST and IST EDRs for each sensor channel. (Sounding channel families around 50-60 and 183 GHz are listed as groups. Channels that are neither H or V pol. are not needed by the ST algorithm.) Channels that are applied to each EDR retrieval are marked either as required to meet or approach threshold requirements (X) or used to meet or approach objectives (O). Additional channels above 18 GHz can enhance performance.

Table 3-3: Instrument Characteristics (833 km altitude is default)

	SELECTED SENSOR CHANNEL SPECIFICATIONS								
Channel prefix	6	10	18	23	36	60VL	89	166	183V
Channel suffixes	VH	VH, RL	VH, PM, RL	VH	VH, PM	A…V FFT	VH	V	ABC
Frequency range [GHz]	6.45-6.8	10.6-10.7	18.6-18.8	23.6-24.0	36.0-37.0	50-60	87.0-91.0	164.5-167.5	173.4-193.3
LST EDR channel applications[1]		X	X	X	X	X	X	O	O
50 km composite max/min NRF	--								
IST EDR channel applications[1]			X	X	X	X	X	O	O
25 km composite max/min NRF	--	--							
Single-sample NEDT [K]	0.47	1.2	1.3	1.1	0.66	2.8[2]	0.57	2.7	2.7[2]
Cross-scan EFOV [km]	67.7	45.5	23.5	23.5	16.7	14.9	15.3	14.6	16.1
Along-scan EFOV [km]	39.3	24.8	15.5	15.5	10.3	8.2	8.1	8.8	9.0
Integration time [ms]	5	2.5	1.2	1.2	1.2	1.2	1.2	1.2	1.2
Along-scan sample spacing [km]	16.3	8.78	3.82	3.82	4.08	4.08	4.08	4.05	4.05
Cross-scan IFOV [km]	67.7	45.5	23.4	23.4	16.6	15.0	15.6	14.6	16.1
Along-scan IFOV [km]	37.8	24.2	15.3	15.3	9.9	7.7	7.8	8.4	8.7
Scan arc designation	A	B	C	C	A	A	A	D	D
Lookdown angle	46.98	48.70	45.40	45.40	47.00	47.01	46.99	46.85	46.86
Earth incidence angle	55.76	58.16	53.63	53.63	55.79	55.81	55.77	55.58	55.60
Field of regard [deg.]	127	113	145	145	127	127	127	129	129
833 km altitude swath width for sample centers [km]	1760	1754	1745	1745	1750	1751	1750	1751	1754
816 km altitude swath width for sample centers [km]	1719	1714	1707	1707	1710	1711	1709	1713	1714

[1] X = channel required to meet or approach threshold; O = channel used to meet or approach objectives.
[2] Figures are for lowest frequency in set. For illustrative purposes only.

3.8. Requirements for cross sensor data (NPOESS or other sensors)

The present design of the ST algorithm does not require any data from sensors other than CMIS.

3.9. Required, alternate, and enhancing algorithm inputs

3.9.1. CMIS data and product requirements

Table 3-4: Inputs from other CMIS algorithms

CMIS Products	Usage
Effective Temperature from Core Module Algorithm	-Primary LST and IST EDR retrieval input -Required at 25 and 50 km HCS
Spectral Emissivity from Core Module Algorithm	-For ice concentration estimation (IST EDR only) -Required at 18V, 18H, and 36V at 25 km HCS -Required at current time
Precipitation Flag from Core Module Algorithm	-Quality control input -Required at current time, 25 and 50 km HCS

3.9.2. Other NPOESS Sensor Data and Product Inputs

No sensor data or products are required from other NPOESS instruments.

3.9.3. External Data Requirements

Table 3-5: External data requirements

External Data	Usage
Surface Database	-Provides static surface data indicating if cell is land and if so if it is ice -Provides static surface data for land fraction inputs used in ice concentration estimation. Data indicates fraction of cell covered by an applicable water body (ocean or selected fresh water bodies) such that remaining fraction is composed of land or non-applicable water bodies

3.9.4. Alternate and Enhancing Data Sources

Table 3-6: Alternate and enhancing data sources

Data Source	Usage
CMIS: 18V, 18H, 23V, 36V, 36H, 89V, and 89H TBs	-Alternatives to spectral emissivity inputs

4. Algorithm description

4.1. Theoretical description of algorithm

The ST algorithm's primary input is surface temperature retrieved by the CMIS Core Physical Inversion Module. The *ATBD for the Core Physical Inversion Module* (AER, 2000) describes this process in more detail. The Core Module removes atmospheric effects and retrieves surface effective emitting temperature T_{eff} and spectral emissivity e from top-of-atmosphere brightness temperature measurements. The Core Module uses a plane parallel model of the atmosphere whose lower boundary condition is parameterized by T_{eff} and e, where $e \equiv 1 - r$ and r is the surface specular reflectivity. The Core Module flags precipitation and passes atmospheric retrieval quality control values that are used by the ST algorithm.

For each retrieval, the Core Module uses two empirically-derived statistical control parameters to constrain the state solution space: The "background" which is a vector of mean values for each model variable including emissivities and surface temperature; and the covariance matrix whose diagonal elements are the variance values for each model variable and whose off-diagonal elements are the inter-variable covariances. For temperature and atmospheric variables, the background/covariance set is based on statistics calculated for an air mass type or region determined by air mass pre-classification or geolocation, respectively. (See the *ATBD for the Core Module* for more details on pre-classification from brightness temperatures.) When deriving LST or IST, the Core Module uses geolocation to determine if the surface is land or ocean; if land, it uses geolocation to choose the surface emissivity background/covariance set associated with non-ice land or ice-covered land; if ocean, it uses brightness temperature pre-classification to choose the emissivity background/covariance set associated with open ocean or ocean with sea ice cover. The algorithm also maintains a dynamic database of day-to-day geolocated surface emissivities derived from CMIS retrievals. This database can be used to make a tightly constraining emissivities background/covariance set to be applied where the temporal change in emissivity is small. More details on background/covariance selection are provided in the *ATBD for the Core Module.*

For IST retrieval, the algorithm also uses emissivity inputs to estimate the ice concentration, as described in the *ATBD for Ice EDRs*. The algorithm's estimate of IST from the mean cell temperature using (9) is based on a linear mixing model for the surface-emitted brightness temperature of a cell with N surface types:

$$T_{Bs} = \sum_{N} f_i T_{eff,i} e_i \tag{10}$$

where f_i is the fractional coverage of surface i, T_{eff} is the temperature, and e is the emissivity. All the ice types in a cell are assumed to have the same temperature.

4.2. Mathematical Description of Algorithm

The following processing steps occur prior to ST algorithm module execution and are described in other documents: Derivation of CMIS brightness temperatures from raw data (*ATBD for SDR Processing*, AER, 2000); footprint matching and interpolation in the sensor reference frame (*ATBD for Common EDR Processing Tasks*, AER, 2000); Core Module retrievals of surface emissivities and effective emitting temperature (*ATBD for the CMIS Core Physical Inversion Module*, AER, 2000); and mapping of sensor-gridded data to an earth-grid (*ATBD for Common EDR Processing Tasks*, AER, 2000).

Each of the following sections provides a mathematical description of a component of the CMIS ST algorithm. Some trivial components (namely, programming logic) are excluded. See Figure 4-1 for a processing flow diagram. Note that all of the coefficients and constants are tunable parameters whether or not they are given an explicit value here.

Land surface temperature

As noted above, the LST EDR product is equivalent to the earth-gridded value of the effective (or skin) surface temperature product of the atmospheric Core Module retrieved at 50 km HCS. The ST algorithm module assigns this value to the LST EDR.

Ice concentration

The *ATBD for the Ice EDRs* describes the derivation of first year sea ice, multi-year sea ice, and fresh water ice concentrations from Core Module retrieved 18V, 18H, and 36V emissivities. To estimate ice concentrations at 25 km HCS, the ST algorithm duplicates this process by executing the same ice concentration module with 25 km emissivity inputs.

Ice surface temperature

Given the concentration of each ice type f_i and open water f_w in a 25 km IST retrieval cell, the ST algorithm estimates the ice surface temperature as:

$$T_{ice} = \frac{e_m T_m - f_w e_w T_{w0}}{\sum_{ice} f_i e_i} . \tag{11}$$

where e_m and T_m are Core Module-estimated mean cell emissivity and temperature inputs, the f are fractional coverage estimates discussed above, e_i and e_w are algorithm parameters representing the expected mean ice and water emissivities, and T_{w0} represents expected water

temperature. The algorithm may evaluate (11) using emissivities from any one or multiple channels available at 25 km HCS. The baseline choice (one channel, 37V) is subject to future calibration.

4.3. Algorithm Processing Flow

4.3.1. Processing flow for CMIS surface temperature algorithm

Figure 4-1 shows the processing flow for the ST algorithm to retrieve the LST and IST EDRs. Section 4.1 describes algorithm physics and section 4.2 gives the algorithm's mathematical description. Note that no connections to the 20 km HCS fresh water ice and sea ice EDR retrievals is shown because the ST algorithm executes an ice concentration calculation separately at 25 km HCS for the IST product.

Figure 4-1: Surface temperature algorithm processing flow diagram

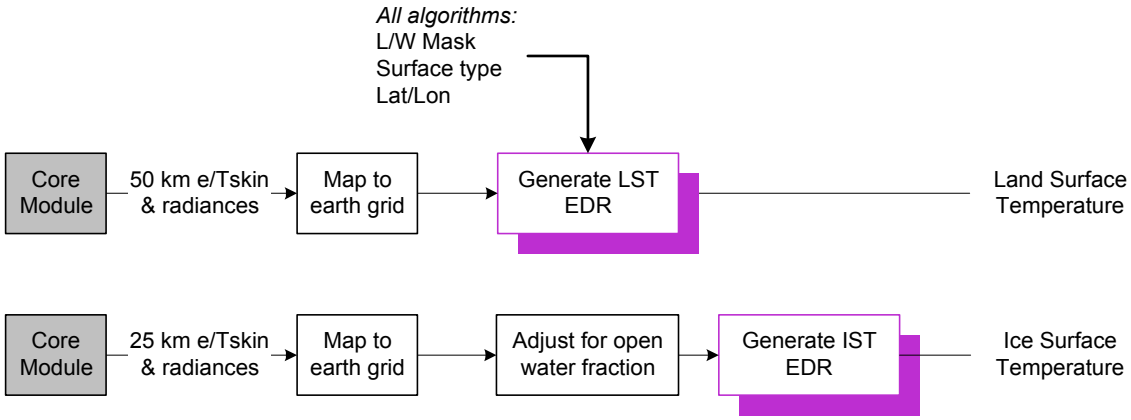

4.4. Algorithm inputs

The table below summarizes the input data used by the ST algorithm. Input data requirements are described in more detail in section 3.9.

Table 4-1: ST algorithm – Input data description

Input Data	Range
Effective emitting temperature	213-343 K
Emissivities @ 18V, 18H, and 36V	0-1
Static surface type	One of {ice covered land, non-ice land, ocean}
Land fractions	0-1 land (non-water body)
Precipitation flag	One of {0,1}

4.5. Algorithm products

The tables below summarize the characteristics of the operational ST algorithm products.

Table 4-2: LST – Operational Product Description

Parameter	Value
Range	213-343 K
HCS	50 km
Units	K
QC Flag	Low Quality Input Data, Missing Data

Table 4-3: IST – Operational Product Description

Parameter	Value
Range	~213-275 K
HCS	25 km
Units	K
QC Flag	Low Quality Input Data, Missing Data

5. Algorithm Performance

5.1. General Description of Nominal and Limited Performance Conditions

This section describes the nominal and limited performance conditions at which the threshold requirements can be achieved. Two SRD sections address special conditions. SRDC3.2.1.1.1-4: "In the event the requirements for an EDR cannot be fully satisfied, the contractor shall identify the requirements which are not fully satisfied, and specify the conditions when they will not be satisfied." SRDC3.2.1.1.1-5: "The contractor shall also specify the conditions under which it recommends delivering an EDR which is incomplete and/or of degraded quality, but which is still of potential utility to one or more users."

The following tables describe the conditions under which nominal predicted performance can be achieved.

Table 5-1: LST – Nominal performance characteristics

Conditions needed to meet threshold requirements	Description	Comments/Characteristics
Atmospheric condition	• Clear or cloudy • Precipitation < 1 mm/hr	Precipitation blocks signal from surface

Table 5-2: IST – Nominal performance characteristics

Conditions needed to meet threshold requirements	Description	Comments/Characteristics
Atmospheric condition	• Clear or cloudy • Precipitation < 1 mm/hr	Precipitation blocks signal from surface
Ice concentration	• Ice concentration > 80%	Open water contaminates ice temperature signal

The following table describes the Limited Performance Characteristics under specific conditions; nominal predicted performance may not be entirely achieved under these conditions.

Table 5-3: LST – Performance under limited performance conditions

Conditions	Description	Comments/Characteristics
Precipitation	Precipitation > 1 mm/hr	No retrieval

Table 5-4: IST – Performance under limited performance conditions

Conditions	Description	Comments/Characteristics
Precipitation	Precipitation > 1 mm/hr	No retrieval
Moderate ice concentration	Ice concentration >50% and <95%	Limited retrieval (degraded uncertainty)
Low ice concentration	Ice concentration <50%	Limited retrieval (severely degraded uncertainty)

5.2. Measurement performance estimates

This section details type performance estimates for each performance metric assigned to the algorithm from the following SRD attributes: *Horizontal Cell Size, Measurement Range,* and either *Measurement Accuracy* and *Measurement Precision* (for LST) or *Measurement Uncertainty* (for IST). The Core Module's algorithm simulation environment (described in detail in the *ATBD for the Core Module*) is the basis for all quantitative performance estimates for these attributes. The simulation environment matches atmospheric profiles to surface emissivity sets, generates simulated brightness temperatures at CMIS channels for each match, then applies the Core Module retrieval algorithm.

- For the LST measurement error performance figures reported here, 400 profile-emissivity matches were made per surface class (summarized in Table 5-5) with profiles having below-freezing surface temperatures matched only to the snow and ice class and profiles having above-freezing surface temperatures matched only to the forest, shrubland, and barren classes. (The snow and ice class contains an equal number of simulated snow-on-land and ice cases.) The algorithm was configured to select a background-covariance constraint based on geolocation (ice cases only) or on a brightness temperature check for high-emissivity surfaces. The possible background-covariance sets were limited to sea ice, land ice, high-emissivity land, and global-land.
- For IST, 400 profile-emissivity matches were made per sea ice and land ice cases. Only profiles with below-freezing surface temperature were used. The algorithm used geolocation to select either a land-ice or sea-ice background-covariance constraint set.

Of the remaining attributes, *Horizontal Reporting Interval* (in addition to *Horizontal Cell Size*) is derived from the spatial properties of the sensor footprints, footprint compositing and interpolation performance, and grid definition; *Horizontal Coverage* is satisfied through the spacecraft orbit specification and algorithm definitions (that is, the LST retrieval is performed over land and the IST retrieval is performed over land and sea ice by definition), *Mapping Uncertainty* is satisfied by spacecraft stability and instrument pointing error requirements, and *Swath Width* is met primarily through spacecraft orbit and instrument specifications and footprint compositing and interpolation performance. For related algorithm performance assessments, see the *ATBD for Footprint Matching and Interpolation* and the *ATBD for Common EDR Processing Tasks*. Note that Horizontal Cell Size is an explicit part of the assessment of the measurement error metrics. That is, quantitative performance estimates represent comparisons of retrieved products and true cell-average products.

5.2.1. Binning Categories

Measurement error performance is stratified by reporting performance in bins. Each bin represents a range of values for a particular environmental condition, or category, including the retrieved parameter itself (e.g., surface temperature). IST categories are land ice, sea ice, and surface temperature. LST categories are land ice, sea ice, surface temperature, and the three land surface types summarized in Table 5-5 along with their assumed annual global occurrence rates. As indicated in the table, emissivity is used as a surface type discriminator because the error

metrics of many of the Core Module retrieval products vary with it. The representative surface type associated with each range identifies the true surface type of the region from which the test emissivities were drawn. Only selected types are used because we found that LST performance varied little among the surface types falling within a particular emissivity range. Note that for sub-freezing temperatures only snow and ice cases were tested whereas for above freezing temperatures snow and ice were excluded.

Table 5-5: 18V emissivity range, representative surface type, and global annual rate of condition occurrence

Emissivity	0.9-1	0.86-0.9	0.8-0.86	<0.8
Representative surface type	Mixed forest	Open shrubland	Barren	Snow and ice
Occurrence [%]	54.3	13.6	16.9	15.2

5.2.2. Horizontal Cell Size Performance

The CMIS horizontal cell size is the size of a square cell to which the derived EDR value is assigned and against which the EDR product is validated. For LST, algorithm performance predictions below are based on the required HCS of 50 km and 50 km is therefore the characteristic HCS of the EDR; similarly for IST, performance predictions are base on a 25 km HCS. 30 km is the required HCS for IST. Since IST uncertainty estimates at 25 are only marginally worse than at 30 km and IST is the only CMIS EDR required at 30 km HCS, we chose to use 25 km HCS and eliminate the need for any data processing or Core Module runs at the 30 km cell size.

5.2.3. LST Measurement Precision and Measurement Accuracy Performance

The following tables summarize predicted LST measurement precision and accuracy stratified by surface temperature. Section 5.3 describes the measurement error budget and assumptions in more detail. Note that the required performance is given in accordance with the accuracy and precision interpretations outlined in section 3.4.2.

Table 5-6: LST predicted measurement precision

Measurement precision [K]	Mean cell surface temperature range [K]								Overall
	Sub-freezing surfaces (ice and snow)				Other surface types				
	<242	242-252	253-264	>264	<280	280-290	290-300	>300	
Budget total	1.89	2.16	2.42	2.46	2.19	1.80	1.61	2.17	1.99
Requirement	<2.5	<2.5	<2.5	<2.5	<2.5	<2.5	<2.5	<2.5	<2.5

Table 5-7: LST predicted measurement accuracy

Measurement accuracy [K]	Mean cell surface temperature range [K]								Overall
	Sub-freezing surfaces (ice and snow)				Other surface types				
	<242	242-252	253-264	>264	<280	280-290	290-300	>300	
Budget total	0.49	0.18	0.24	0.21	0.23	0.11	0.46	0.41	0.30
Requirement	<0.5	<0.5	<0.5	<0.5	<0.5	<0.5	<0.5	<0.5	<0.5

5.2.4. IST Measurement Uncertainty

The following table summarizes predicted IST measurement uncertainty stratified by surface temperature and land and sea ice categories. Section 5.3 describes the measurement error budget and assumptions in more detail.

Table 5-8: IST predicted measurement uncertainty

Measurement uncertainty [K]	Mean cell surface temperature range [K]				Overall
	<242	242-252	253-264	>264	
Requirement	<1	<1	<1	<1	<1
Budget (land)	2.89	2.59	3.00	3.04	2.88
Budget (ocean)	2.12	2.75	2.92	2.83	2.65

5.2.5. Measurement Range Performance

By algorithm definition, surface temperature measurement range is unlimited. (Quality control will flag failed or non-physical retrievals.) The performance estimates above delineate the measurement error predictions for IST and LST. The LST measurement requirements are met in all temperature ranges. Nominal IST measurement uncertainty (3 K) is met in all IST temperature bins.

5.3. Sensitivity Studies

The tables below give the error budget derivation for our LST and IST measurement error predictions summarized above. The baseline errors are from simulation test results described in detail in the *ATBD for the Core Module* and include atmospheric effects, natural emissivity variability, sensor calibration and measurement noise errors, and atmospheric algorithm retrieval errors. (See also EN #83 response.) Additional errors are budgeted for the following sources:

- Footprint and cell mismatch: Errors due to the fact that more than 40% of the composite footprint weight falls outside of the EDR retrieval cells. No additional error in this category is added at this time.
- Heterogeneity: Errors due to spatial temperature, emissivity, and atmospheric heterogeneity in the retrieval cell. Errors from this source are assumed to be negligible except for IST retrievals over sea ice. In this case strong correlation between temperature and emissivity (i.e., from leads in the ice pack) may cause significant errors even with the open water correction applied. (See test results stratified by open water fraction below.)

Table 5-9: LST measurement precision error budget

Measurement precision [K]	Budget action	Mean cell surface temperature range [K]								Overall
		Sub-freezing surfaces (ice and snow)				Other surface types				
		<242	242-252	253-264	>264	<280	280-290	290-300	>300	
Global tests	Baseline est.	1.74	2.03	2.30	2.34	2.19	1.80	1.61	2.17	1.97
Footprint & cell mismatch	Adds to error	0	0	0	0	0	0	0	0	0.00
Heterogeneity	Adds to error	0	0	0	0	0	0	0	0	0.00
Gradients	Adds to error	0.75	0.75	0.75	0.75	0	0	0	0	0.11
Budget total	Sqrt. sum sqrs.	1.89	2.16	2.42	2.46	2.19	1.80	1.61	2.17	1.99
Requirement		<2.5	<2.5	<2.5	<2.5	<2.5	<2.5	<2.5	<2.5	<2.5

Table 5-10: LST measurement accuracy error budget

Measurement accuracy [K]	Budget action	Mean cell surface temperature range [K]								Overall
		Sub-freezing surfaces (ice and snow)				Other surface types				
		<242	242-252	253-264	>264	<280	280-290	290-300	>300	
Global tests	Baseline est.	0.99	0.18	0.24	0.21	0.23	0.11	0.56	0.51	0.36
Footprint & cell mismatch	Adds to error	0	0	0	0	0	0	0	0	0.00
Heterogeneity	Adds to error	0	0	0	0	0	0	0	0	0.00
Bias calibration	Reduces error	-0.5	0	0	0	0	0	-0.1	-0.1	-0.06
Budget total	Sum errors	0.49	0.18	0.24	0.21	0.23	0.11	0.46	0.41	0.30
Requirement		<0.5	<0.5	<0.5	<0.5	<0.5	<0.5	<0.5	<0.5	<0.5

Table 5-11: IST measurement uncertainty error budget — land ice

Measurement uncertainty [K]	Budget action	Mean cell surface temperature range [K]			
		<242	242-252	253-264	>264
Land ice tests	Baseline est.	2.71	2.39	2.83	2.87
Footprint & cell mismatch	Adds to error	0	0	0	0
Heterogeneity	Adds to error	0	0	0	0
Gradients	Adds to error	1	1	1	1
Budget total	Sqrt. sum sqrs.	2.89	2.59	3.00	3.04
Requirement		<1	<1	<1	<1

Table 5-12: IST measurement uncertainty error budget — sea ice

Measurement uncertainty [K]	Budget action	Mean cell surface temperature range [K]			
		<242	242-252	253-264	>264
Sea ice tests	Baseline est.	1.80	2.51	2.70	2.60
Footprint & cell mismatch	Adds to error	0	0	0	0
Heterogeneity	Adds to error	1	1	1	1
Gradients	Adds to error	0.5	0.5	0.5	0.5
Budget total	Sqrt. sum sqrs.	2.12	2.75	2.92	2.83
Requirement		<1	<1	<1	<1

Table 5-12 shows detailed stratification of the so-called heterogeneity error stratified by open water fraction. (In this table, baseline sea ice test results are the average over all temperature bins given above.) Heterogeneity error is added to one-dimensional test results to account for correlated temperature and emissivity variability across the retrieval cell—that is, the error due to the imperfect open water fraction correction (9). The error was estimated using the sea ice simulation environment described in the *ATBD for the Ice EDRs*. Heterogeneity error is non-zero even when open water fraction is zero because the correction (9) is executed using retrieved ice concentrations with non-zero retrieval errors. Note that in the budget table above, 1 K is allocated to heterogeneity error which effectively means that open water coverage fractions from 0-0.2 are accommodated by the nominal performance estimates. (See also EN #63 response.)

Figure 5-1: IST sea ice measurement uncertainty stratified by open water fraction

Measurement uncertainty [K]	Budget action	Open water coverage fraction					
		0	0-0.2	0.2-0.4	0.4-0.6	0.6-0.8	0.8-0.9
Sea ice tests	Overall avg.	2.40	2.40	2.40	2.40	2.40	2.40
Footprint & cell mismatch	Adds to error	0	0	0	0	0	0
Heterogeneity	Adds to error	0.73	0.9	1.6	2.66	5.1	13.87
Gradients	Adds to error	0.50	0.50	0.50	0.50	0.50	0.50
Budget total	Sqrt. sum sqrs.	2.56	2.61	2.93	3.62	5.66	14.09

Figure 5-2 shows LST measurement precision budget totals stratified by surface type. Sea ice, land ice, and snow-on-land were tested with temperature profiles having above-freezing surface temperature. Mixed forest, open shrubland, and barren types were tested with below-freezing surface temperatures only. Performance for land ice and snow is worse due primarily to higher variance in the surface emissivity and commensurate inter-channel decorrelation as well as the additional error budget allocations for surface temperature gradients listed above.

Figure 5-2: LST measurement precision by surface type

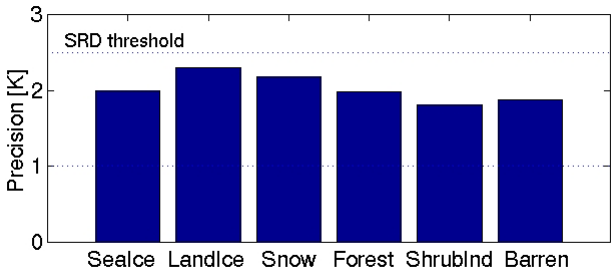

Figure 5-3 shows the sensitivity of IST predicted performance to a change in the algorithm channel set that eliminates 18 and 22 GHz channels. Note that all predictions include error budget allocations for surface temperature gradients as detailed in the budget tables above. The exercise shows about 1 K RMS additional error incurred when the 18 and 22 GHz channels are removed. What is not accounted for is the error *reduction* potentially realized by removing the lowest frequency channels in the IST channel set. Since ice and snow penetration depths may be more than twice as large at 18 than 36 GHz—for example, 2.7 vs. 1.4 cm in homogeneous sea ice and 2.7 vs. 1.4 m (sic) in pure fresh ice—surface vertical temperature gradients mean that the effective emitting temperatures at each channel may be significantly different. This is problematic both because it violates the Core Module's assumption that all channels have the same emitting temperature and because the retrieval's goal is to measure temperature as close to the surface as possible. Consequently, the option to remove 18 and 22 GHz channels from the IST retrieval may have a net benefit on retrieval performance if the temperature gradient-induced error realized with the channels in place exceeds the error of removing the channels. CMIS calibration/validation or tests with similar sensor data can be used to fully evaluate the 18-22 GHz removal option.

Figure 5-3: IST measurement uncertainty budget with "full" and "No18/22" CMIS channel set (see text)

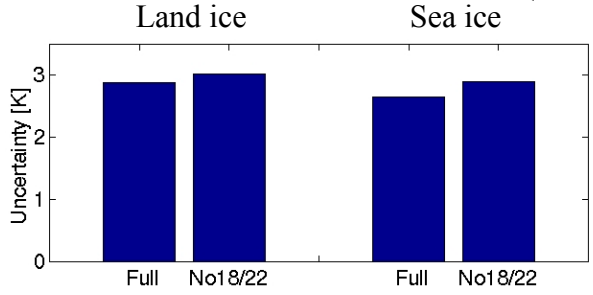

5.4. Constraints, Limitations, and Assumptions

- Measurement performance predictions are predicated on the assumptions summarized in the error budget tables above.
- Baseline measurement performance predictions are based on simulations using regional/global emissivity background/covariance data. Potential benefits of a dynamic emissivity database are not included. A dynamic emissivity database may improve performance where temporal emissivity variance is small by providing a tight constraint on emissivity based on several recent CMIS emissivity retrievals. Conversely, performance may be degraded when an emissivity change occurs but goes undetected by the algorithm.

5.5. Algorithm performance tests with similar sensor data

We have tested the surface temperature algorithm with data similar to CMIS from the SSM/I and TMI sensors. The objectives of the tests were to demonstrate consistent and robust retrieval operability with a real-data stream. The limited atmospheric sounding capability of SSM/I and TMI—both have only one channel, 22 GHz, falling on an atmospheric absorption feature—means that quantitative retrieval tests with these instruments are not good predictors of CMIS retrieval performance. The test described in the following paragraphs compares emissivities retrieved by the Core Module from SSM/I brightness temperatures to emissivities independently derived using SSM/I and ancillary atmospheric and surface temperature data (Prigent et al., 1998). Because correct Core Module emissivity retrieval is a prerequisite for accurate surface temperature retrieval, the ability of the Core Module to retrieve emissivity is a good surrogate for surface temperature performance. This test shows good correspondence between the Core Module's emissivities and the reference emissivity dataset.

5.5.1. Emissivity retrieval from SSM/I

Prigent et al. (1998) has derived global emissivity datasets at the SSM/I channels: 19.35V/H, 22.235V, 37V/H, and 85.5V/H GHz. Global emissivity maps at selected channels are given in the *ATBD for the Vegetation/Surface Type EDR*. Prigent used a radiative transfer model to calculate emissivity given atmospheric and surface parameters. Data from ISCCP (International Satellite Cloud Climatology Project) analyses of visible and infrared satellite observations provided cloud detection and surface skin temperature estimates at the 30 km resolution of the ISCCP DX datasets. NCEP reanalysis provided atmospheric profiles at 2.5° resolution in latitude and longitude. Emissivity is derived for cloud-free and thin, high cloud cells in the DX data sets where SSM/I and ancillary data are available. Monthly average emissivity and its standard deviation for July and October, 1992, are reported for each cell with a sufficient number of retrievals per month. The July and October datasets contain 184,223 and 185,419 non-ocean reports, respectively, with an additional 114,659 and 115,272 ocean reports covering high latitudes only.

Surface temperature and atmospheric parameters are the primary error sources in the emissivity database. Prigent et al. (1997) estimates that the ISCCP surface temperature estimation error is ≤ 2 K which leads to an emissivity retrieval error estimate ≤ 0.007 (per observation) assuming no atmosphere, 0.9 emissivity, and 258 K surface temperature. As an indication of atmospheric errors, the monthly average standard deviation over all land reports is 0.018 at 19V and 0.021 at 22V suggesting at least 0.01 additional RMS error contribution due to atmospheric effects at 22 and 85 GHz and less at 37 GHz. Other error sources include mismatched geolocation, spatial resolution, and temporal sampling between SSM/I and ancillary observations. On average, each emissivity report is based on about 33 observations per month with a commensurate reduction in random errors. Residual systematic errors include a fixed IR emissivity assumption, local reanalysis bias, and observation timing. Based on this analysis, we assume that the net emissivity characterization error or the dataset is about 0.005-0.01.

The Prigent dataset is a good surrogate for CMIS-retrieved emissivities in performance testing for several reasons. Firstly, it represents most of the useful spectral range of CMIS that will be available for 20 km HCS retrieval. Second, its measurement uncertainty is comparable to or greater than that expected for CMIS emissivities at the same channels (~0.005). Lastly, the Prigent dataset is globally representative and covers two months at the peak and declining stages of the Northern Hemisphere vegetation cycle.

5.5.2. Testing procedure

SSM/I data for October, 1992, were collected for the contiguous United States, Mexico, and parts of Canada. About 30 observations per point were acquired. The Core Module was applied to each observation and the monthly average and standard deviation of emissivities for each point were calculated. The Core Module was configured to use a single fixed background-covariance set representing a broad range of emissivity spectra. (In fact, emissivity data derived earlier by Prigent et al., 1997, for Africa were used to build the covariance set applied here.)

5.5.3. Test results

Figure 5-4 and Figure 5-5 show maps of reference (from the Prigent dataset) and Core Module-retrieved emissivities at 19 GHz H and V-polarizations, respectively. In both plots the Core Module emissivities have almost the same spatial distribution as the Prigent data. The Core Module emissivities are generally slightly lower than the Prigent emissivities and this may be consistent with a positive bias in the Prigent data due to the assumption of infrared emissivity equal to 1 in her emissivity derivations: Over-estimated IR emissivity leads to underestimated surface temperatures and consequently higher microwave emissivity estimates (e.g., $e \propto T_B/T_{\mathrm{IR}}$). The Prigent and Core Module monthly emissivity standard deviations are also similar—about 0.02 at 19V and 0.025 at 19H.

Figure 5-4: Reference (top) and Core Module (bottom) 19H emissivities, mean-monthly, October, 1992

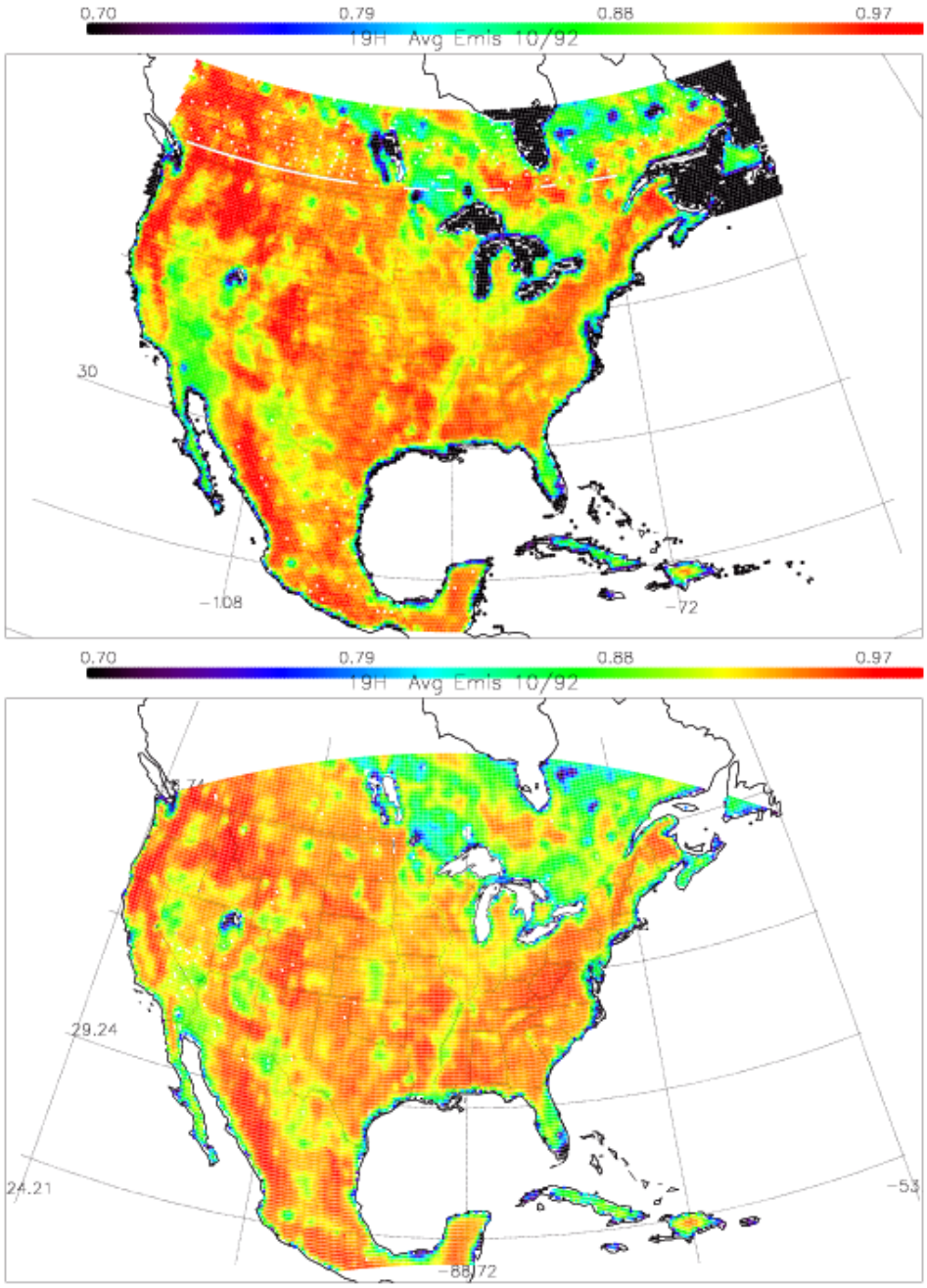

Figure 5-5: Reference (top) and Core Module (bottom) 19V emissivities, mean-monthly, October, 1992

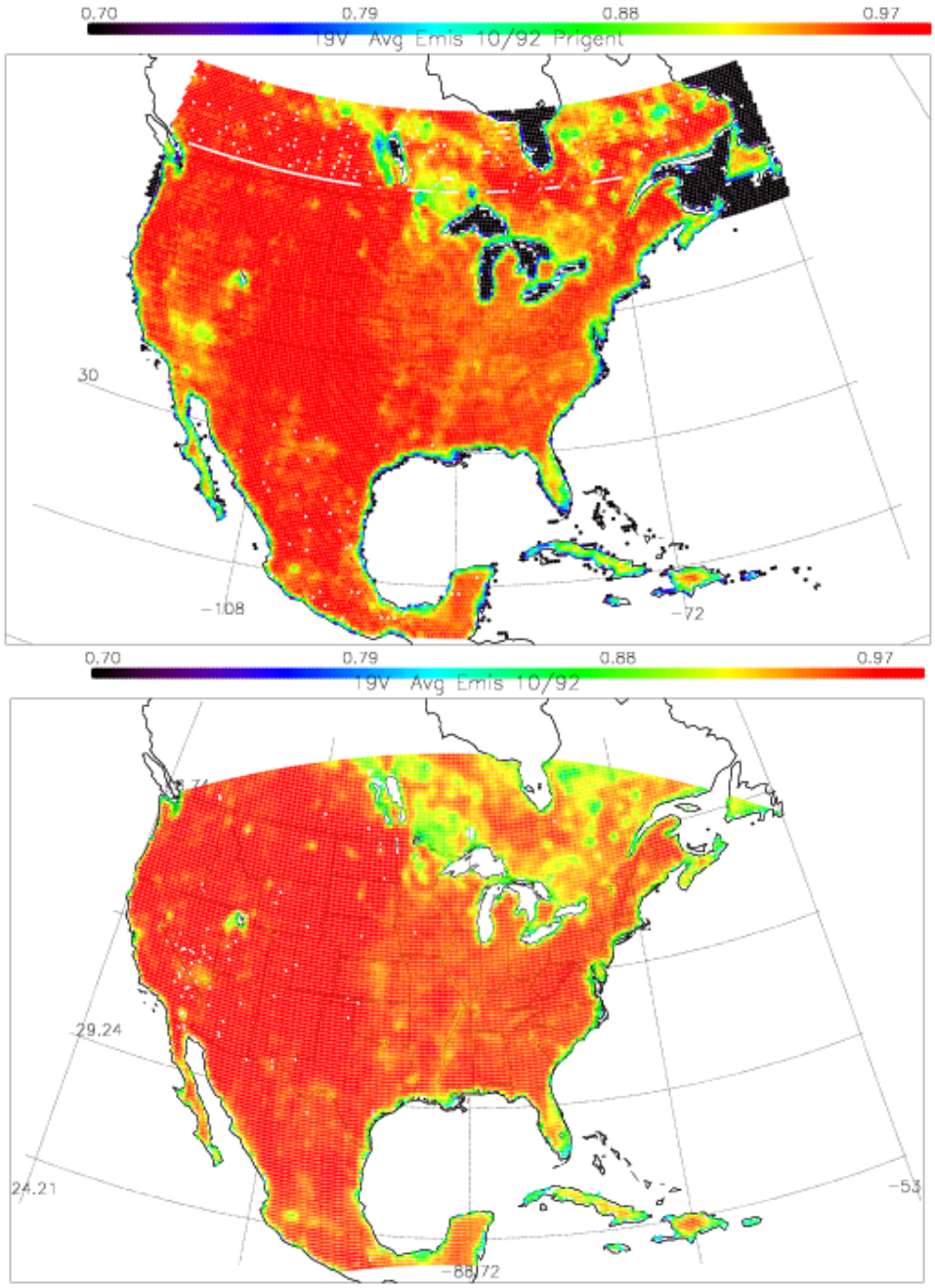

6. Algorithm Calibration and Validation Requirements

6.1. Pre-launch

To be completed.

6.2. Post-launch

To be completed.

6.3. Special considerations for Cal/Val

To be completed.

6.3.1. Measurement hardware
To be completed.

6.3.2. Field measurements or sensors
To be completed.

6.3.3. Sources of truth data
To be completed.

7. Practical Considerations
7.1. Numerical Computation Considerations
To be completed.

7.2. Programming/Procedure Considerations
To be completed.

7.3. Computer hardware or software requirements
To be completed.

7.4. Quality Control and Diagnostics
To be completed.

7.5. Exception and Error Handling
To be completed.

7.6. Special database considerations
To be completed.

7.7. Special operator training requirements
To be completed.

7.8. Archival requirements
To be completed.

8. Glossary of Acronyms

AMSR	Advanced Microwave Scanning Radiometer
ATBD	Algorithm Theoretical Basis Document
AVHRR	Advanced Very High Resolution Radiometer
BT	Brightness Temperature [K]
CMIS	Conical Microwave Imaging Sounder
DEM	Digital Elevation Model
DMSP	Defense Meteorological Satellite Program
EDR	Environmental Data Record
EIA	Earth Incidence Angle
ESMR	Nimbus-7 Electrically Scanning Microwave Radiometer
FOV	Field Of View
IFOV	Instantaneous Field Of View
LST	Land Surface Temperature [K]
NPOESS	National Polar-orbiting Operational Environmental satellite System
RFI	Radio-Frequency Interference

RMS	Root Mean Square
RMSE	Root Mean Square Error
SDR	Sensor Data Record
SSM/I	Special Sensor Microwave/Imager
SSMIS	Special Sensor Microwave Imager Sounder
TB	Brightness Temperature
TMI	TRMM Microwave Imager
TOA	Top-of-Atmosphere (i.e., measured by sensor)
TRMM	Tropical Rainfall Measuring Mission
USGS	United States Geological Survey
VIIRS	Visible/Infrared Imager/Radiometer Suite
VIRS	Visible and Infrared Radiometer System (on TRMM)
VST	Vegetation/Surface Type
VWC	Vegetation Water Content [kg/m2]

9. References

9.1. Technical Literature

Basist, A., N. C. Grody, T. C. Peterson, and C. H. Williams, Using the Special Sensor Microwave/Imager to monitor land surface temperature, wetness, and snow cover, *J. Appl. Meteor.*, 37:888-911, 1998.

Gloersen, P., W. J. Campbell, D. J. Cavalieri, J. C. Comiso, C. L. Parkinson, and H. J. Zwally, *Arctic and Antarctic Sea Ice, 1978-1987: Satellite Passive-Microwave Observations and Analysis*, NASA SP No. 511, 1993.

McFarland, M. J., R. L. Miller, and C. M. U. Neale, Land surface temperature derived from the SSM/I passive microwave brightness temperatures, *IEEE Trans. Geosci. Rem. Sens.*, 28(5):839-845, 1990.

Njoku, E. G., Surface temperature estimation over land using satellite microwave radiometry, in *Passive Microwave Remote Sensing of Land Atmosphere Interactions*, B. J Choudhury, Y. H. Kerr, E. G. Njoku, and P. Pompalone, eds., VSP, Utrecht, 1995.

Prigent, C., W. B. Rossow, and E. Matthews, Microwave land surface emissivities estimated from SSM/I observations, *J. Geophys. Res.*, 102(D18):21867-21890, 1997.

Prigent, C., W. B. Rossow, E. Matthews, Global maps of microwave land surface emissivities: Potential for land surface characterization, *Radio Science,* 33(3):745-751, 1998.

Steffen, K., J. Key, D. J. Cavalieri, J. Comiso, P. Gloersen, K. St. Germain, I. Rubinstein, The estimation of geophysical parameters using passive microwave algorithms, in *Microwave Remote Sensing of Sea Ice*, F. D. Carsey, ed., American Geophysical Union, pp. 51-71: 1992.

St. Germain, K. M., and D. J. Cavalieri, A microwave technique for mapping ice temperature in the Arctic seasonal sea ice zone, *IEEE Trans. Geosci. Rem. Sens.*, 35(4):946-953, 1997.

Weng, F., and N. C. Grody, Physical retrieval of land surface temperature using the special sensor microwave imager, *J. Geophys. Res.,* 103(D8):8839-8848, 1998.

Williams, C. N., A. Basist, T. C. Peterson, and N. Grody, Calibration and verification of land surface temperature anomalies derived from the SSM/I, *Bull. Am. Meteor. Soc.*, 81(9):2141-2156, 2000.